

# DEUTSCHES ELEKTRONEN-SYNCHROTRON DESY

DESY 74/14  
April 1974



$\pi^0$ -Electroproduction on Hydrogen Near Threshold  
at Four-Momentum Transfers of 0.2, 0.4 and 0.6 GeV<sup>2</sup>

by



P. Brauel, F.-W. Büsler, Th. Canzler, D. Cords, W. R. Dix, R. Felst,  
G. Grindhammer, W.-D. Kollmann, H. Krehbiel, J. Meyer and G. Weber

*Deutsches Elektronen-Synchrotron DESY, Hamburg*  
*and*

*II. Institut für Experimentalphysik der Universität Hamburg*

2 HAMBURG 52 . NOTKESTIEG 1

To be sure that your preprints are promptly included in the  
HIGH ENERGY PHYSICS INDEX ,  
send them to the following address ( if possible by air mail ) :

DESY  
Bibliothek  
2 Hamburg 52  
Notkestieg 1  
Germany

$\pi^0$ -Electroproduction on Hydrogen Near Threshold at Four-Momentum Transfers  
of 0.2, 0.4 and 0.6  $\text{GeV}^2$

by

P. Brauel, F.-W. Büsser\*, Th. Canzler, D. Cords, W.R. Dix, R. Felst,  
G. Grindhammer, W.-D. Kollmann, H. Krehbiel, J. Meyer and G. Weber

Deutsches Elektronen-Synchrotron DESY, Hamburg, Germany,

and

II. Institut für Experimentalphysik der Universität Hamburg

Abstract

The reaction  $e + p \rightarrow e + \pi^0 + p$  was measured near the one pion threshold, detecting the final electron and proton in coincidence for values of  $q^2 = 0.2, 0.4$  and  $0.6 \text{ GeV}^2$ . The slope of the cross section at threshold is determined. The data are compared with those of the  $e + p \rightarrow e + \pi^+ + n$  reaction, measured simultaneously, and with the results of pseudovector Born approximation and with dispersion theoretical calculations.

---

\*Present address: CERN, Geneva, Switzerland

We report on an experiment, in which the reactions

$$e + p \rightarrow e + n + \pi^+ \quad (1)$$

$$\text{and } e + p \rightarrow e + p + \pi^0 \quad (2)$$

were studied at squared four-momentum transfers of  $q^2 = 0.2, 0.4$  and  $0.6 \text{ GeV}^2$  and at invariant masses  $W$  of the pion-nucleon system between threshold and  $1.13 \text{ GeV}$ . From the results of reaction (1), published previously<sup>1)</sup>, we deduced, within a theoretical framework based on PCAC and current algebra, values of the axial vector nucleon form factor. For this analysis, the Born-term-model of ref. 2, with pseudovector pion-nucleon coupling, was used. The same model, without contact and pion exchange term, also predicts the cross section of reaction (2) near threshold. The results for reaction (2) therefore provide a check on the validity of some of the theoretical assumptions on which the model of reference 2 is based. In the following we present the cross section of reaction (2) and compare the data with those of reaction (1) as well as with the results of the pseudovector Born approximation<sup>2)</sup> and dispersion theoretical calculations<sup>3,5)</sup>.

The differential cross section of reactions (1) or (2) in the one photon exchange approximation is given by<sup>3)</sup>

$$\frac{d^3\sigma}{dE' d\Omega_e d\Omega_\pi^*} = \Gamma_t \frac{W|\vec{p}^*|}{E_\gamma M} \left[ W_1 + \varepsilon W_4 + \varepsilon \sin^2\theta^* \cos 2\phi^* W_2 + \sqrt{\frac{\varepsilon(\varepsilon+1)}{2}} \sin\theta^* \cos\phi^* W_3 \right] \quad (3)$$

where the polarization parameter  $\varepsilon$  and the virtual photon flux parameter  $\Gamma_t$  are defined as usual (see ref.3).  $E'$  is the energy of the scattered electron and  $E_\gamma = (W^2 - M^2)/2M$ , where  $M$  is the proton mass. Quantities denoted by an asterisk are given in the CMS of the outgoing hadrons.  $\vec{p}^*$  is the pion momentum and  $\theta^*$  and  $\phi^*$  are, respectively, the polar- and azimuthal angles of the  $\pi$  in a

right handed coordinate system with the three-momentum vector of the virtual photon pointing in the positive z-direction and with  $\vec{p} \times \vec{p}'$  in the positive y-direction, where  $\vec{p}$  and  $\vec{p}'$  are the momenta of the incident and the scattered electron, respectively. In general the structure functions  $W_i$  are functions of  $W$ ,  $q^2$  and  $\theta^*$ ; they are defined above as the slope of a cross section with respect to  $|\vec{p}^*|$ . Since the measurements were performed at a fixed value of  $\epsilon$  of about 0.98, no separation of  $W_1$  and  $W_4$  was possible in this experiment. Considering contributions only of s- and p-waves in the  $\pi$ -N-system, which is a good approximation in the kinematic range of the present experiment, the  $\theta^*$ -dependence of the  $W_i$  can be specified as:

$$\begin{aligned} W_1 + \epsilon W_4 &= \bar{A}_0 + \bar{A}_1 \cos\theta^* + \bar{A}_2 \cos^2\theta^* \\ W_2 &= C_0 \\ W_3 &= D_0 + D_1 \cos\theta^* \end{aligned} \quad (4)$$

The angular coefficients  $\bar{A}_0$ ,  $\bar{A}_1$ ,  $C_0$ ,  $D_0$ ,  $D_1$  were determined in the experiment assuming  $\bar{A}_2$  to be known theoretically.

The ( $n \pi^+$ ) and ( $p \pi^0$ ) channels were measured simultaneously and the experimental set up was identical to the one described in ref.1. Electrons scattered at an angle of  $8.5^\circ$  were detected together with the coincident protons, whose flight direction was measured by a  $9 \times 6$  array of large volume plastic scintillation counters. The proton detection efficiency of this counter system was about 90%. It was calibrated via elastic (e-p)-scattering. Only protons going backward in the CMS at  $q^2 = 0.2 \text{ GeV}^2$  were of too short a range to be registered. To reduce the background due to the reaction  $e + p \rightarrow e + p + \gamma$ , the recoil protons of this process were detected by a counter telescope viewing the target at an appropriate angle. At the  $q^2$ - and  $W$ -values of the present experiment the solid angle of this telescope did not overlap with the one of the recoil

nucleons of reactions (1) and (2).

The data analysis was very similar to the one described in ref.1. It was performed by comparing the measured proton rates in each of the various nucleon detector elements with the analogous rates calculated by Monte Carlo techniques. In these calculations the cross section of Eq.(3) was integrated over the acceptances of the electron spectrometer and of the various nucleon detector elements using the angular coefficients (4) as parameters. Corrections due to radiative processes (Eq.4.1 of ref.4) and due to the efficiency and the resolution of the nucleon detector were folded into the theoretical cross section (Eq.(3)). The measured and the theoretical distributions were compared using the  $\chi^2$ -method, and the angular coefficients were determined by minimizing the  $\chi^2$ -function. In order to keep errors small,  $\bar{A}_2$  was inserted from theory, and only the angular coefficients  $\bar{A}_0$ ,  $\bar{A}_1$ ,  $C_0$ ,  $D_0$ ,  $D_1$  were treated as free parameters. Separate fits were made for each W bin.

In Fig. 1 the angular coefficients obtained from the fits are plotted versus W for the  $q^2 = 0.6 \text{ GeV}^2$  measurements as an example. Fits for two different sets of  $\bar{A}_2$  values are shown.  $\bar{A}_2 \equiv 0$  and  $\bar{A}_2$  as calculated by v. Gehlen and Wessel<sup>5)</sup> are used ( $\bar{A}_2 = 0.0, -0.2, -0.6 \text{ } \mu\text{b/sr}$  at  $W = 1.080, 1.10, 1.12 \text{ GeV}$  respectively are the values). The coefficients  $C_0$ ,  $D_0$  and  $D_1$  turn out to be independent of  $\bar{A}_2$ , and  $\bar{A}_0$  is only weakly correlated with  $\bar{A}_2$ . The error bars in Fig. 1 do not include an overall normalisation error of about 4% and the errors due to the uncertainties of the W scale. The curves shown in Fig. 1 which are the results of a dispersion theoretical calculation by v. Gehlen and Wessel<sup>5)</sup> fit the data quite well within the errors. The  $q^2 = 0.2$  and  $0.4 \text{ GeV}^2$  data show the same qualitative features. The full results will be published elsewhere.

The integrated cross section for each channel is given by

$$\frac{d^2\sigma}{dE' d\Omega_e} = \Gamma_t \frac{W |\vec{p}^*|}{E_\gamma M} 4\pi \Sigma \quad (5)$$

$$\Sigma = \bar{A}_0 + \frac{1}{3} \bar{A}_2 \quad (6)$$

The quantity  $\Sigma$  was found to be independent of our assumptions about  $\bar{A}_2$ .

This is to be expected since in the present experiment the integrated cross section (5) is measured almost independently of the angular distribution (4).

The quantity  $\Sigma$ , which is plotted versus  $|\vec{p}^*|^2$  in Fig. 2, is therefore proportional to the slope of the integrated cross section. For comparison the  $\Sigma$  values obtained from the  $\pi^+$  data<sup>1)</sup> are shown in Fig. 2 together with those from positive<sup>6,7)</sup> and neutral<sup>8,9)</sup> pion photoproduction. The error bars shown include the statistical and normalisation errors except for the error due to the uncertainty of the  $W$  scale, which is correlated for both channels and is listed separately in Table 1. Threshold values were obtained by fitting a straight line

$$\Sigma = \Sigma^{\text{thr}} + B |\vec{p}^*|^2 \quad (7)$$

to the data points. The numerical values of  $\Sigma^{\text{thr}}$  are listed in Table 1. The  $q^2$  dependence of  $\Sigma^{\text{thr}}$  and  $B$  for the  $(\pi^0 p)$  channel is shown in Fig. 3.

Also shown are the photoproduction values<sup>8)</sup> and the results of the Frascati<sup>11)</sup> and the Daresbury<sup>10)</sup> experiments. In the latter the  $(p \pi^0)$ -channel was not measured directly but the data were obtained by subtracting the  $(n \pi^+)$ -channel from the total cross section. The curves shown are calculated in Born Approximation using pseudoscalar (PSBA) and pseudovector (PVBA) pion nucleon couplings and proton form factors given by the relations

$$G_M^P(q^2)/\mu_p = G_E^P(q^2) = (1 + q^2/0.71)^{-2}.$$

Summarizing our results we conclude the following:

a) The slope of the  $\pi^0$  cross section at threshold

$$\Sigma^{\text{thr}} = \lim_{|\vec{p}^*| \rightarrow 0} \frac{M E_\gamma}{4\pi \Gamma_t W |\vec{p}^*|} \frac{d^2\sigma}{d\Omega_e dE'} \quad \text{is small and compatible with 0.}$$

b) Near threshold the ratio  $\Sigma^{\pi^0} / \Sigma^{\pi^+}$  increases with increasing  $q^2$ . The data even indicate that  $\Sigma^{\pi^0}$  near threshold rises with increasing  $q^2$  reaching a maximum at about  $q^2 = 0.3 \text{ GeV}^2$ .

c) Within the errors the dispersion theoretical calculations of v. Gehlen and Wessel<sup>5)</sup> fit the  $\pi^0$  data quite well. The pseudovector Born Approximation results are consistent with the values of  $\Sigma^{\text{thr}}$  measured in the present experiment. Therefore its application is justified for the case of  $\pi^+$  electroproduction.

In preparing, running and evaluating the experiment we enjoyed the wholehearted support of the floor service, synchrotron and computer groups. We want to thank Dr. D. Harms and P.E. Kuhlmann for their help in the early phases of the experiment and Messrs. H. Bebermeier, R. Ehrenfort, E. Gadermann, J. Gauerky and K. Sauerberg for their assistance during the measurements. The authors are grateful for advice given by Prof. G.V. Gehlen, Dr. F. Gutbrod and Dr. B.J. Read concerning theoretical questions.



$q^2$ (GeV <sup>2</sup> )	$e + p \rightarrow e + n + \pi^+$		$e + p \rightarrow e + p + \pi^0$	
	$\Sigma^{\text{thr}}$ ( $\mu\text{b}/\text{sr}$ )	error ( $\mu\text{b}/\text{sr}$ ) uncorrelated   correlated	$\Sigma^{\text{thr}}$ ( $\mu\text{b}/\text{sr}$ )	error ( $\mu\text{b}/\text{sr}$ ) uncorrelated   correlated
0.2	6.55	$\pm 0.82$   $\pm 0.70$	0.09	$\pm 0.66$   $\pm 0.50$
0.4	2.50	$\pm 0.53$   $\pm 0.50$	0.15	$\pm 0.31$   $\pm 0.60$
0.6	1.91	$\pm 0.38$   $\pm 0.40$	0.36	$\pm 0.27$   $\pm 0.50$

Table 1

Threshold values  $\Sigma^{\text{thr}}$  as a function of  $q^2$ . The total errors are split into uncorrelated errors and errors which are correlated between both channels. The latter are mainly due to the uncertainty of the W scale.

References

- 1) P. Brauel, F.-W. Büsser, Th. Canzler, D. Cords, W.R. Dix, R. Felst, G. Grindhammer, W.-D. Kollmann, H. Krehbiel, J. Meyer, G. Weber;  
Phys. Letters 45B (1973) 389
- 2) N. Dombey, B.J. Read; Nucl. Phys. B60, 65 (1973)
- 3) G. v. Gehlen; Nucl. Phys. B9 (1969) 17 and Nucl. Phys. B20 (1970) 102
- 4) Y.S. Tsai; SLAC-PUB-848 (1971)
- 5) G.v. Gehlen, H. Wessel; Bonn Univ. PI 2-94 (1971)
- 6) M.I. Adamovich, V.G. Larinova, R.A. Latypova, S.P. Kharlamov, F.R. Yagudina; Sov. Journal of Nucl. Phys. 7, (1968) 643
- 7) M.I. Adamovich, V.G. Larinova, A.I. Lebedev, S.P. Kharlamov, F.R. Yagudina; Sov. Journal of Nucl. Phys. 2 (1966) 95
- 8) B.B. Govorkov, S.P. Denisov, E.V. Minarik;  
Sov. Journal of Nucl. Phys. 4 (1967) 265
- 9) W. Hitzeroth; Nuovo Cimento 60A (1969) 467
- 10) D.R. Botterill, D.W. Braben, P.R. Norton, A. Del Guerra, A. Giazotto M.A. Giorgi, A. Stefanini;  
Lett. Nuov. Cim., 8, 910, (1973)
- 11) E. Amaldi, B. Borgia, P. Pistilli, M. Balla, G.V. Di Giorgio, A. Giazotto, S. Serbassei, G. Stoppini; Nuovo Cimento 65A (1970) 377
- 12) J.C. Alder, F.W. Brasse, E. Chazelas, W. Fehrenbach, W. Flauger, K.H. Frank, E. Ganssauge, J. Gayler, V. Korbel, J. May, M. Merkwitz, A. Courau, G. Tristam, J. Valentin;  
Nucl. Phys. B46 (1972) 573

Figure Captions

Fig. 1) Angular coefficients obtained from the fits to the  $q^2 = 0.6 \text{ GeV}^2$  data are plotted versus  $W$  for two different sets of  $\bar{A}_2$ . The results coincide where only one symbol is plotted. The curves drawn are from the dispersion theoretical calculation of ref. 5. The data of Alder et al.<sup>12)</sup> are plotted for comparison.

Fig. 2)  $\Sigma$  of the  $(n \pi^+)$  and  $(p \pi^0)$  channels versus  $|\vec{p}^*|^2$ .  $\Sigma$  is proportional to the slope of integrated cross section. The photoproduction values are plotted for comparison. The extrapolated threshold values are specially indicated.

Fig. 3) The threshold value  $\Sigma^{\text{thr}}$  and the slope  $B$  of  $\Sigma$  determined from the  $\pi^0$  data of the present experiment versus  $q^2$ . The full errors are shown. Results of the experiments at Frascati<sup>11)</sup> and Daresbury<sup>10)</sup> are also shown as well as the photoproduction value<sup>6,7,8,9)</sup>. The curves drawn are the results obtained from the Born terms only, using pseudoscalar (PSBA) and pseudovector (PVBA) pion nucleon coupling.

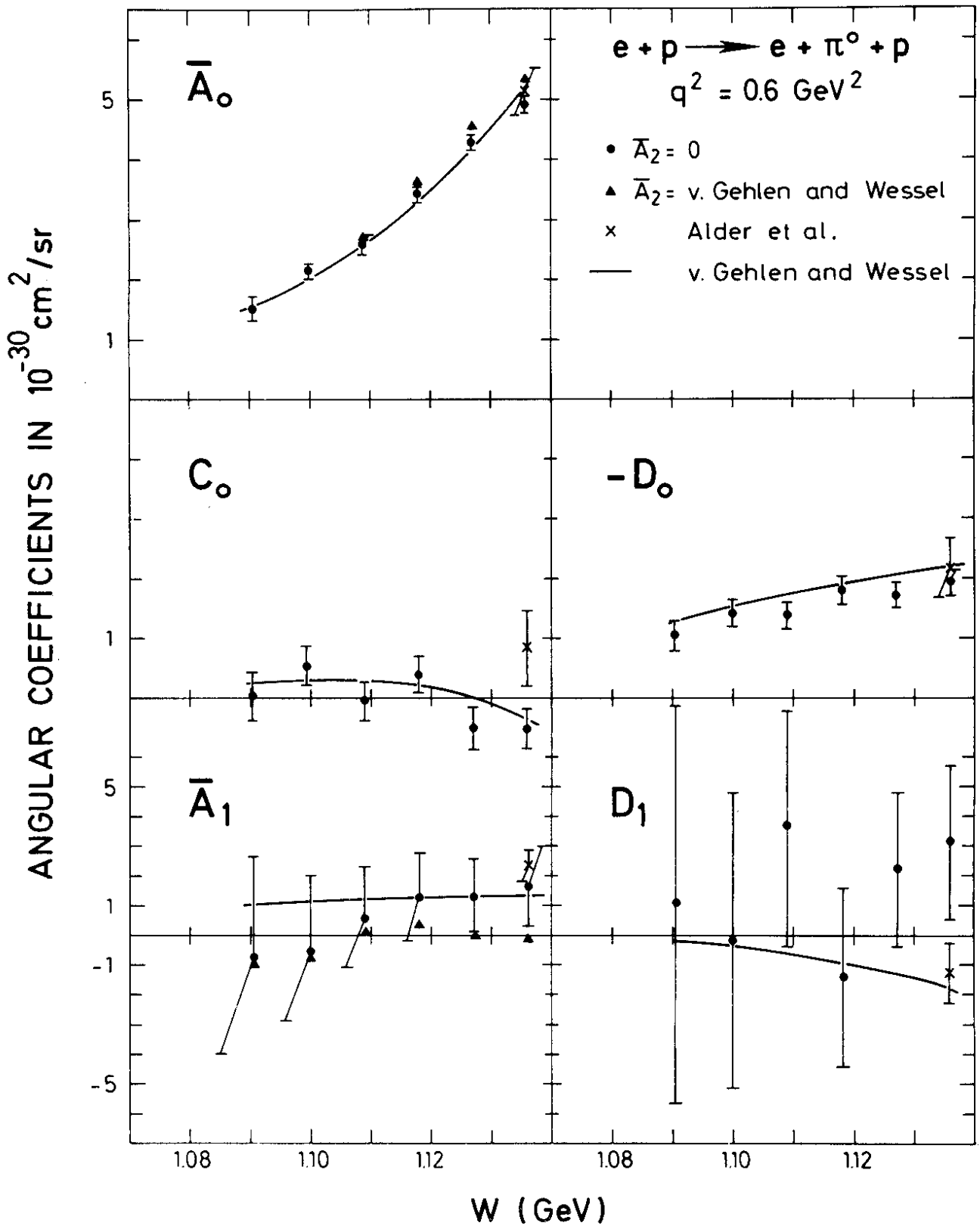


Fig. 1

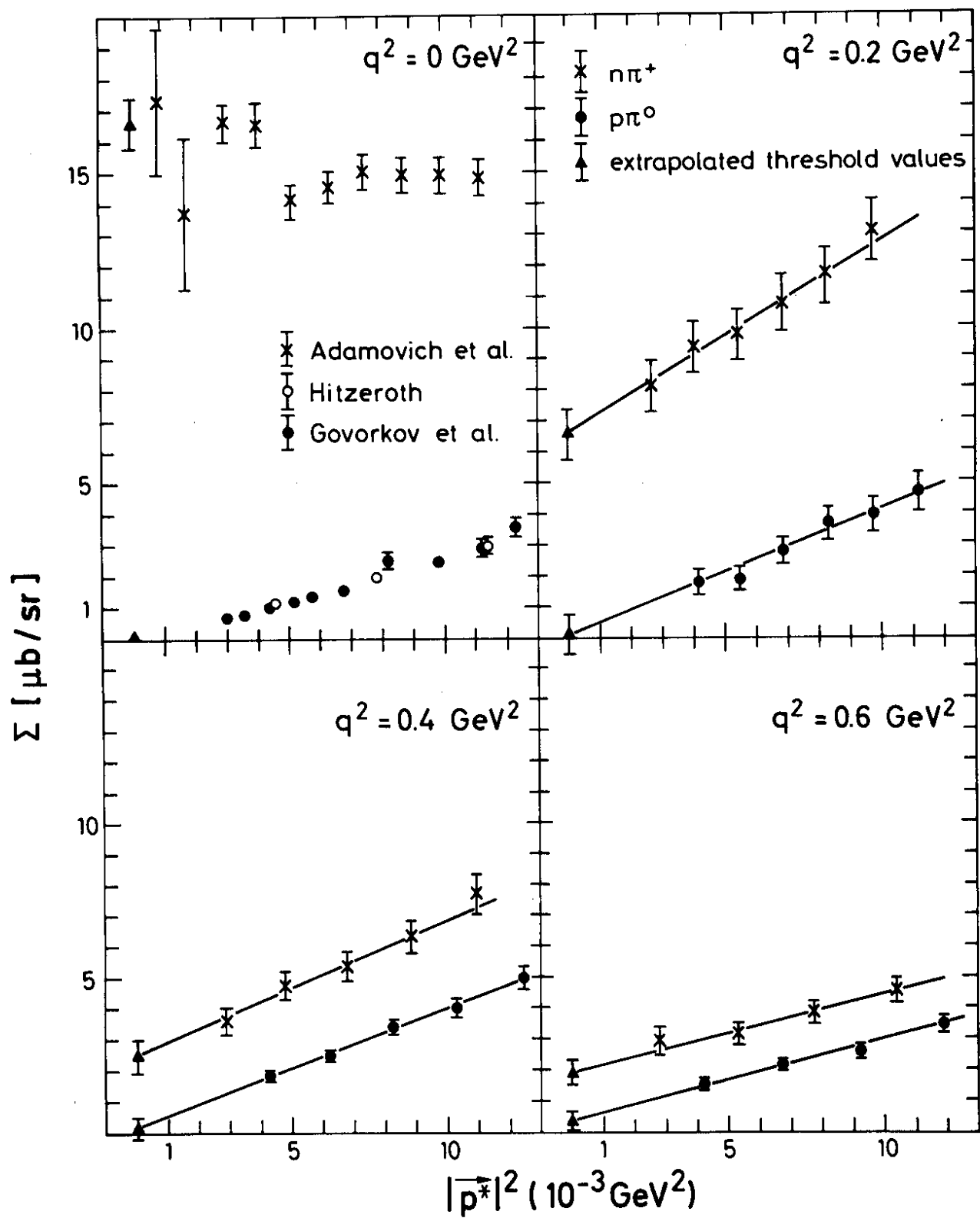


Fig. 2

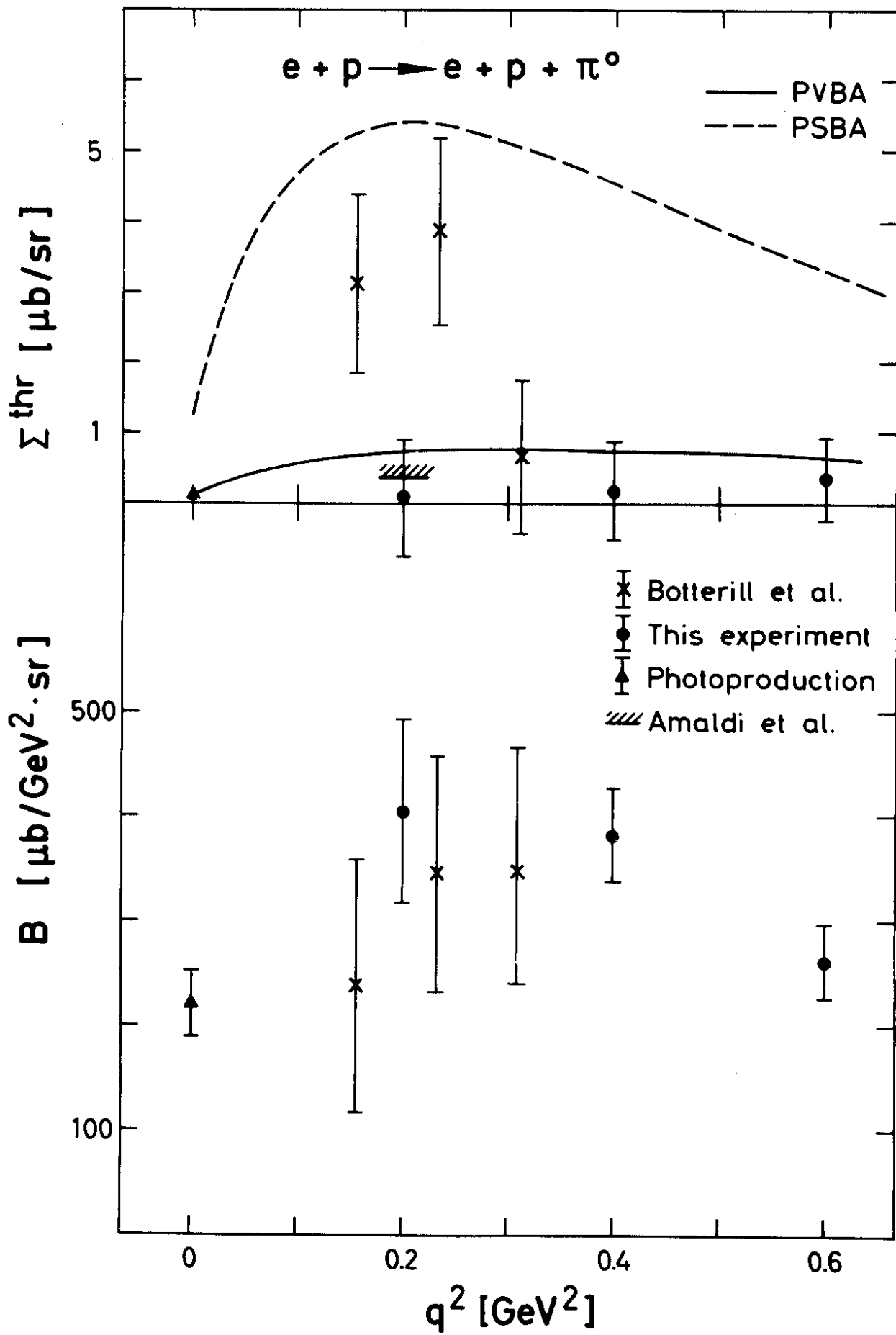


Fig. 3